Notes on Numerical Fluid Mechanics
and Multidisciplinary Design 139

David Anderson · Pierre-Etienne Gautier
Masanobu Iida · James T. Nelson
David J. Thompson · Thorsten Tielkes
David A. Towers · Paul de Vos
Jens C. O. Nielsen *Editors*

Noise and Vibration Mitigation for Rail Transportation Systems

Proceedings of the 12th International Workshop on Railway Noise, 12–16 September 2016, Terrigal, Australia

Springer

Notes on Numerical Fluid Mechanics and Multidisciplinary Design

Volume 139

Notes on Numerical Fluid Mechanics and Multidisciplinary Design publishes state-of-art methods (including high performance methods) for numerical fluid mechanics, numerical simulation and multidisciplinary design optimization. The series includes proceedings of specialized conferences and workshops, as well as relevant project reports and monographs.

More information about this series at http://www.springer.com/series/4629

David Anderson · Pierre-Etienne Gautier
Masanobu Iida · James T. Nelson
David J. Thompson · Thorsten Tielkes
David A. Towers · Paul de Vos
Jens C. O. Nielsen
Editors

Noise and Vibration Mitigation for Rail Transportation Systems

Proceedings of the 12th International Workshop on Railway Noise, 12–16 September 2016, Terrigal, Australia

Springer

ISSN 1612-2909 ISSN 1860-0824 (electronic)
Notes on Numerical Fluid Mechanics and Multidisciplinary Design
ISBN 978-3-319-73410-1 ISBN 978-3-319-73411-8 (eBook)
https://doi.org/10.1007/978-3-319-73411-8

Library of Congress Control Number: 2018933008

Printed on acid-free paper

This Springer imprint is published by the registered company Springer International Publishing AG part of Springer Nature
The registered company address is: Gewerbestrasse 11, 6330 Cham, Switzerland

Preface

This volume contains the peer-reviewed contributions to the 12th International Workshop on Railway Noise (IWRN12), which took place in Terrigal, Australia, on 12–16 September 2016. The workshop was hosted by the Australian Acoustical Society (AAS, the Australian professional body for those working in acoustics) in partnership with the Asset Standards Authority (ASA, the design and standards authority within Transport for NSW).

IWRN12 was also made possible by the support of the primary sponsors for the event: Pandrol Track Systems (Gold sponsor), Delkor Rail (Silver sponsor) and Vossloh Fastening Systems (Bronze sponsor).

The workshop was attended by 135 delegates and 11 accompanying persons from 16 countries: Australia (53), China (19), UK (11), Japan (11), Belgium (6), USA (5), Singapore (5), Germany (5), France (5), Sweden (4), Canada (3), Austria (2), Switzerland (1), Spain (1), South Africa (1) and the Netherlands (1).

In comparison with other modes of transportation, rail transport is safe and environmentally friendly and is generally described as the most sustainable mode for regional and international transport. However, it is also recognised that the environmental impact of railway noise and vibration needs to be further reduced. Since the first IWRN in 1976, held in Derby (UK) with 35 delegates, the workshop series has been established as a regular event (held every three years) that brings together the leading researchers and engineers in all fields related to railway noise and vibration. The IWRN workshops have contributed significantly to the understanding and solution of many problems in railway noise and vibration, building a scientific foundation for reducing environmental impact by air-borne, ground-borne and structure-borne noise and vibration.

Following the tradition from previous workshops, the scientific programme of IWRN12 was held as a single-session event (no parallel sessions) over three and a half days. The programme contained 54 oral presentations and 25 poster presentations. The poster sessions commenced with a series of two-minute oral presentations to introduce each paper, and these sessions were very well attended.

This volume contains the peer-reviewed papers from 61 of these presentations, including two state-of-the-art papers on curve noise and on policy, regulation and perception. IWRN12 covered eight different themes: High-Speed Rail and Aerodynamic Noise; Interior Noise; Policy, Regulation and Perception; Predictions, Measurements and Modelling; Rail Roughness, Corrugation and Grinding; Squeal Noise; Structure-Borne Noise, Ground-Borne Vibration and Resilient Track Forms; and Wheel and Rail Noise.

In parallel with the scientific programme, 11 companies gathered at IWRN12 to display their technology and services in the area of railway noise and vibration: Pandrol Track Systems; Delkor Rail; Brüel & Kjær; ETMC Technologies; JSG Industrial Systems; Marshall Day Acoustics; LB Foster/Airlube Australasia; Pyrotek; Schrey & Veit; SoundScience and Wilson Acoustics.

There is no formal organisation behind the IWRN but rather an informal, committed International Committee. It supports the chairman during the preparation process with the experience and expertise of its members. Assistance is given to formulate the scientific programme by reviewing the submitted abstracts, to act as session chairmen and to act as peer review group and editors of the IWRN proceedings published in this volume.

The International Committee is grateful to David Hanson for his diligent work in organising the scientific programme and to Kym Burgemeister, Tom Cockings, Peter Karantonis, Serge Vegh and Conrad Weber of the local committee for their great commitment and care in organising the workshop.

The editors of this volume are grateful to Professor Wolfgang Schröder as the general editor of the "Notes on Numerical Fluid Mechanics and Multidisciplinary Design" and also to the staff of the Springer Verlag (in particular, Dr. Leontina Di Cecco) for the opportunity to publish the proceedings of the IWRN12 workshop in this series. Note that previous workshop proceedings have also been published in this series (IWRN9 in volume 99, IWRN10 in volume 118 and IWRN11 in volume 126).

We hope that this volume will be used as a "state-of-the-art" reference by scientists and engineers involved in solving noise and vibration problems related to railway traffic.

Stanmore, Australia — David Anderson
Paris, France — Pierre-Etienne Gautier
Tokyo, Japan — Masanobu Iida
Emeryville, USA — James T. Nelson
Southampton, UK — David J. Thompson
Munich, Germany — Thorsten Tielkes
Burlington, USA — David A. Towers
Weesp, The Netherlands — Paul de Vos
Gothenburg, Sweden — Jens C. O. Nielsen
June 2017

Contents

Part III Predictions, Measurements and Modelling

Part I
Squeal Noise

A State-of-the-Art Review of Curve Squeal Noise: Phenomena, Mechanisms, Modelling and Mitigation

David J. Thompson, G. Squicciarini, B. Ding and L. Baeza

Abstract Curve squeal is an intense tonal noise occurring when a rail vehicle negotiates a sharp curve. The phenomenon can be considered to be chaotic, with a widely differing likelihood of occurrence on different days or even times of day. The term curve squeal may include several different phenomena with a wide range of dominant frequencies and potentially different excitation mechanisms. This review addresses the different squeal phenomena and the approaches used to model squeal noise; both time-domain and frequency-domain approaches are discussed and compared. Supporting measurements using test rigs and field tests are also summarised. A particular aspect that is addressed is the excitation mechanism. Two mechanisms have mainly been considered in previous publications. In many early papers the squeal was supposed to be generated by the so-called falling friction characteristic in which the friction coefficient reduces with increasing sliding velocity. More recently the mode coupling mechanism has been raised as an alternative. These two mechanisms are explained and compared and the evidence for each is discussed. Finally, a short review is given of mitigation measures and some suggestions are offered for why these are not always successful.

1 Introduction

Curve squeal is an intense tonal noise produced when railway vehicles negotiate sharp curves. It is probably the most annoying type of noise produced by the railway system due to its tonal nature and its high noise levels. It is also highly unpredictable, with a widely differing likelihood of occurrence for nominally identical vehicles, or for same vehicles on different days or even times of day and might be considered to be chaotic rather than deterministic. Anderson et al. [1] indicate that curve squeal is one of the Australian rail industry's top noise miti-

D. J. Thompson (✉) · G. Squicciarini · B. Ding · L. Baeza
Institute of Sound and Vibration Research, University of Southampton,
Southampton SO17 1BJ, UK
e-mail: djt@isvr.soton.ac.uk

D. Anderson et al. (eds.), *Noise and Vibration Mitigation for Rail Transportation Systems*, Notes on Numerical Fluid Mechanics and Multidisciplinary Design 139,
https://doi.org/10.1007/978-3-319-73411-8_1

gation priorities. Moreover, Hanson et al. [2] point out that squeal noise can be seen as a symptom of the deterioration of some aspect of the maintenance or operation of the railway system: insufficient lubrication leading to wear as well as noise; poor rail profiles leading to high stresses; or poorly steering rolling stock leading to increased wear and fuel consumption.

This paper provides a review of curving noise phenomena, mechanisms, models and mitigation measures. The term curve squeal (or screech) may be used to include several different phenomena with a wide range of dominant frequencies and potentially with different excitation mechanisms. Some authors have made a distinction between 'curve squeal', in which the noise is strongly tonal, and the more intermittent, higher frequency noise that is sometimes called 'flanging noise'. Despite this naming convention there is little conclusive evidence that the latter is actually associated with contact at the wheel flange. Rail corrugation can also occur in curves and lead to high noise levels which may be mistaken for curving noise.

Curve squeal is usually associated with the wider field of friction-induced vibration, a field that includes the classic example of the excitation of the violin string by the bow, some forms of tyre/road noise and brake squeal. Rudd [3] described three alternative mechanisms but concluded that the unsteady lateral creepage at the wheel/rail contact is the most likely reason to induce squeal noise. According to Rudd, the falling friction mechanism (described in Sect. 2) leads to unstable vibration of a mode of the wheel; this will grow in amplitude until the non-linearities in the creep forces result in a limit cycle. He also suggested that rail vibration can be neglected in comparison with the vibration of wheel. Rudd's model was also described by Remington at IWRN4 in a review that covered squeal and impact noise [4] as well as rolling noise [5].

The model of Rudd [3], based on the concept of 'falling friction', has formed the basis of many subsequent and more detailed models of curve squeal. However, more recently a number of authors have proposed an alternative mechanism based on 'mode coupling'. The purpose of this paper is to explain these two mechanisms, to review experimental and theoretical work in the field of curve squeal and to discuss mitigation measures in terms of these two mechanisms. The mechanisms are introduced and compared in Sect. 2 on the basis of simple models. Models of curve squeal are reviewed in Sect. 3, measurements on test rigs and in the field are described in Sect. 4 and mitigation measures are discussed in Sect. 5.

2 Frictional Excitation

2.1 Curving Behaviour

Curve squeal can be attributed to 'imperfect' curving behaviour of railway vehicles. The coned wheelset naturally steers around a curve by aligning itself radially to the curve and moving outwards so that the rolling radius difference between the wheels

compensates for the different distances travelled. However, for a bogie (or a two-axle vehicle) the yaw stiffness between the axles and the frame, required to ensure stable running at high speed, prevents the axles from orientating themselves fully radially [6]. Consequently, the wheelsets have a non-zero angle of attack. On sharp curves the leading wheelset of a bogie tends to run in flange contact at the outer wheel whereas the trailing wheelset may run in flange contact at the inner wheel; at higher speeds it moves outwards. The angle of attack is greatest at the leading wheelset, as shown schematically in Fig. 1a.

Due to the non-zero angle of attack, there is a small lateral relative velocity between the wheel and the rail, see Fig. 1b. The relative velocity normalised by the rolling velocity is known as the creepage; components in the longitudinal and spin (rotation about the normal) directions also exist. The lateral creepage is approximately equal to the angle of attack. The creepages give rise to reaction forces known as creep forces. At low values of creepage, the creep force increases linearly with increasing creepage [8]. However, at large values of creepage, such as occurring in sharp curves, the creep force 'saturates' and takes the value of the Coulomb friction coefficient multiplied by the normal load. The ratio of the creep force to the normal load will be referred to here as the adhesion coefficient; in the saturated region it is identical to the friction coefficient. Models for the creep behaviour have been developed by Kalker [8] including the approximate method FASTSIM and the fuller method CONTACT. Vermeulen and Johnson [9] and Shen et al. [10] also give approximate methods.

The importance of friction behaviour on the excitation of squeal noise is widely recognised. To illustrate this, and the basic mechanisms behind it, simple systems are considered in the next sections consisting of a single mode of vibration or a pair of modes.

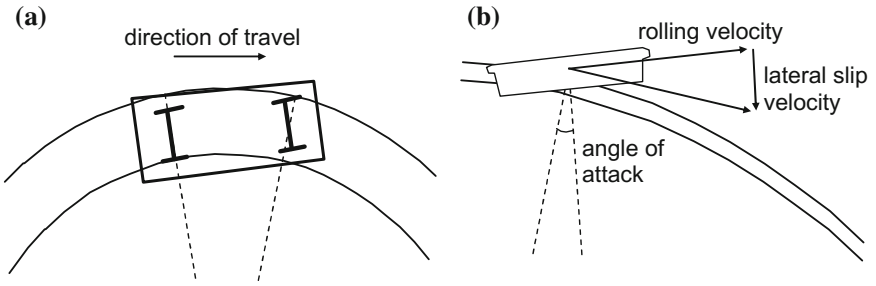

Fig. 1 **a** Typical curving behaviour for small radius curve showing that the leading wheelset has a large angle of attack; **b** generation of lateral creepage by a non-zero angle of attack [7]

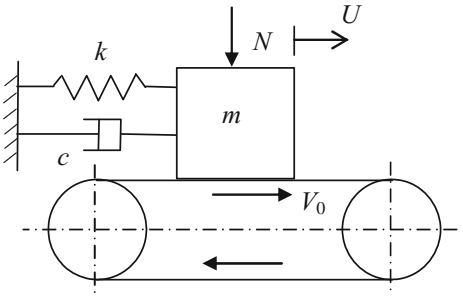

Fig. 2 Schematic view of a restrained mass on a moving belt

2.2 Simple Models of Oscillators with Friction

A simple model that can be used to illustrate stick-slip mechanisms is a mass on a belt moving at velocity V_0, as shown in Fig. 2. The mass m is restrained by a spring of stiffness k and damper c and held against the belt by a constant normal load N. This model can be used to represent a wheel vibrating in a single natural mode (although a wheel has many modes, the squeal response is usually dominated by a single mode). The sliding velocity between the mass and the belt represents the lateral creep velocity (not the rolling velocity), which has a steady-state value of V_0.

In this section we consider friction to be represented by a static coefficient μ_s (when there is no relative motion) and a dynamic coefficient μ_d (when there is slip), with $\mu_s > \mu_d$. In the stick phase the mass moves at the same velocity as the belt and the friction force F satisfies $|F| < \mu_s N$. As the mass moves, the spring is extended until the spring force exceeds the friction limit and sliding commences. The equation of motion for this system satisfies two different conditions, one for the stick phase of the mechanism and one for the slip phase:

$$m\ddot{U} + c\dot{U} + kU = F \quad \text{with} \begin{cases} \dot{U} = V_0, & |F| \le \mu_s N \\ \dot{U} \ne V_0, & |F| = \mu_d N \end{cases} \tag{2.1}$$

where U represents the vibration displacement. During sliding, according to the second equation, the mass undergoes harmonic motion at the natural frequency $\omega_0 = \sqrt{k/m}$. However, due to the existence of the stick phase, the period of oscillation is longer than the natural period associated with the mass-spring system. As shown in [7] the relative importance of the stick and slip phases depends on a non-dimensional parameter

$$\beta = (\mu_s - \mu_d)\frac{N}{V_0 m \omega_0} \tag{2.2}$$

For curve squeal situations the value of β is usually in the range 0.1–1 [7]. Figure 3a shows examples of the stick-slip motion for three values of β. These are shown in the 'phase plane' in which the velocity is plotted against the displacement.

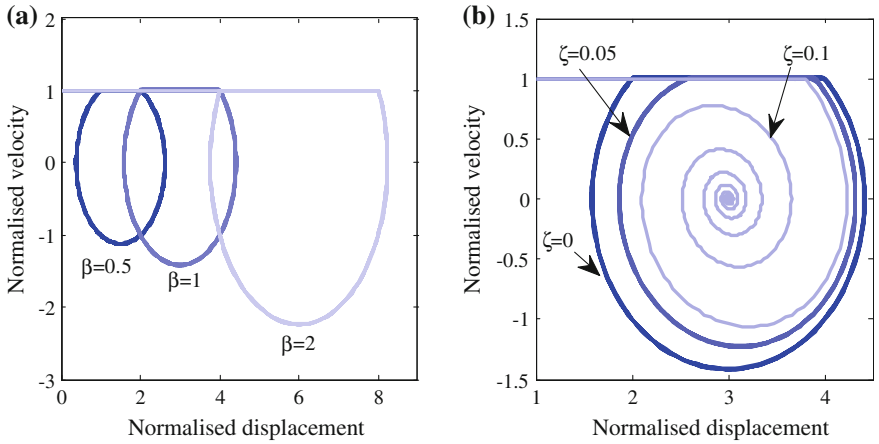

Fig. 3 Normalised displacement versus non-dimensional velocity of a simplified stick-slip mechanism: $\mu_s = 0.4$, $\mu_d = 0.3$. **a** Without damping; **b** for different damping levels ($\beta = 1$)

Here, the velocity is normalised by the belt velocity V_0 whereas the displacement is normalised by V_0/ω_0. These results illustrate the formation of a 'limit cycle': a stable periodic motion that is reached from a variety of initial conditions. It is found that, for small values of β the slip phase predominates, the motion is close to elliptical on the phase plane and the oscillation frequency is close to the natural frequency, whereas for large values of β the stick phase predominates and the oscillation frequency is lower than the natural frequency [7]. Moreover, as the motion is not purely sinusoidal due to the nonlinearity of the friction model, its spectrum will contain higher harmonics in addition to the fundamental frequency, a feature often seen in squeal measurements.

Using this simple model also allows the effect of damping to be assessed. Figure 3b shows results for $\beta = 1$ for three values of damping ratio. As the damping is increased, this has only a small effect on the amplitude of the limit cycle until the damping reaches a value where the oscillations are suppressed; in this case for $\zeta = 0.1$ the damping exceeds the limiting value and the oscillations decay. The limiting value of damping ratio can be approximated as $\zeta > \beta^2/4\pi$ [7].

2.3 Negative Friction Slope Model

As will be seen, the friction coefficient is often found to fall with increasing sliding velocity. The slope of the relation between force and velocity corresponds to a damper (the force due to a damper is proportional to the relative velocity) so a force which falls in magnitude with increasing relative velocity corresponds to a negative damper. If there is a greater negative damping than the positive damping inherent in

the oscillator, unstable self-excited vibration occurs [3], the amplitude of which grows exponentially. In reality, the amplitude is then limited by non-linear effects in the creep force, as there is a region with positive slope close to the origin of the force-creepage relation; see Fig. 4a.

To illustrate this, the single-degree-of-freedom system of the mass on a moving belt can still be adopted to simulate the self-excited vibration of a single wheel mode. Eliminating the steady-state component of the displacement and force, the equation of motion of the system takes the form:

$$\ddot{u} + 2\zeta\omega_0\dot{u} + \omega_0^2 u = -\frac{N}{m}\left(\mu|_{\gamma_0+\gamma} - \mu|_{\gamma_0}\right) \tag{2.3}$$

where $u = U - U_0$ is the dynamic component of the vibration displacement (U_0 is the displacement of the belt moving at speed V_0), ζ is the damping ratio, ω_0 is the natural frequency, N is the load normal to the contact plane, m is the mass, μ is the adhesion coefficient (creep force normalised by the normal load), γ_0 is the lateral creepage at steady state and $\gamma = \dot{u}/V$ is its dynamic component. The right-hand side represents the dynamic component of creep force (normalised by the mass).

For small variations in creepage, the right-hand side of Eq. (2.3) can be linearized:

$$\ddot{u} + 2\zeta\omega_0\dot{u} + \omega_0^2 u = -\frac{N}{mV}\frac{\mathrm{d}\mu}{\mathrm{d}\gamma}\bigg|_{\gamma_0}\dot{u} \tag{2.4}$$

This can be identified as a damping term corresponding to the creep force, which can be compared with the structural damping as a check for stability. Thus if the damping ratio is smaller than

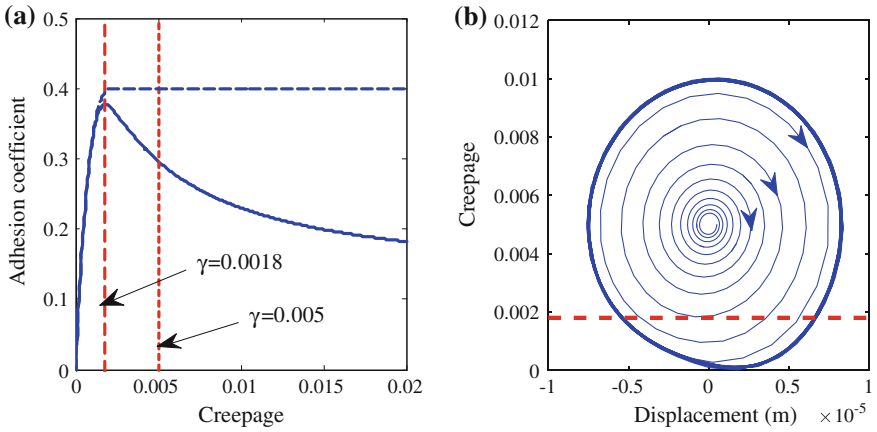

Fig. 4 **a** Normalized creep force from Vermeulen-Johnson [9] (dashed line) and combined with falling part from Huang [11] (solid line); **b** simulation results for a case without damping

$$\zeta_{\text{lim}} = -\frac{N}{2m\omega_0 V}\frac{\mathrm{d}\mu}{\mathrm{d}\gamma}\bigg|_{\gamma_0} \tag{2.5}$$

the system will be unstable and the vibration will grow, whereas for larger values of damping the oscillation will decay. Meanwhile, the solution of the non-linear Eq. (2.3) gives the limit cycle.

The parameters given in Table 1 are adopted in an illustrative simulation and, although arbitrary, they are plausible for a railway wheel. The simplified creep force model proposed by Vermeulen and Johnson [9] is adopted with a falling part as proposed by Huang [11] (see also Sect. 4.1.2). Figure 4a shows the creep force normalised by the normal load (referred to as the adhesion coefficient). Also shown is the corresponding curve obtained with a constant friction coefficient of 0.4. The steady-state creepage is chosen as 0.005. The solution for the undamped system with falling friction is shown in Fig. 4b; the solution grows exponentially until the creepage falls below 0.0018, which corresponds to the value where the slope in Fig. 4a changes sign. For values below this (indicated by the horizontal line in Fig. 4b) the creep force tends to stabilise the system. The limit cycle is reached when the energy fed into the system during the portion of the period corresponding to a falling creep force (overall negative damping) equals the energy dissipated during the time spent in the region with force increasing with creepage (overall positive damping). Clearly, in a situation like this, instability can be avoided by increasing the structural damping above the limit value given in Eq. (2.5). For constant friction there is no instability of this system. According to this model the instability is also independent of the level of static friction.

2.4 Mode Coupling Mechanisms

In addressing curve squeal there is an increase of interest in the direction of mode-coupling phenomena, which have been explained in a simplified form by Hoffmann et al. [12, 13], see also [14]. This type of instability arises from non-conservative displacement-dependent forces and often goes under the name of "flutter". It also occurs in the absence of falling friction. Figure 5a shows the typical system adopted to illustrate this mechanism. Here the mass has two degrees of freedom and two springs. As the mass vibrates, variations in the normal load occur, leading to variations in the friction force. This is also equivalent to the system

Table 1 Parameters of a single mode of the wheel

Modal mass	156 kg	Steady-state creepage, γ_0	0.005
Natural frequency, $\omega_0/2\pi$	1003 Hz	Rolling velocity, V	10 m/s
Normal contact force, N	42 kN	Damping ratio	0

shown in Fig. 5b in which the modes of the wheel may have both vertical and lateral components and the contact angle α of the wheel with the rail may vary.

By considering small oscillations around the equilibrium of steady-state sliding, the system in Fig. 5 can be mathematically described as

$$\begin{bmatrix} m & 0 \\ 0 & m \end{bmatrix} \begin{Bmatrix} \ddot{x} \\ \ddot{y} \end{Bmatrix} + \begin{bmatrix} k_{11} & k_{12} - \mu k_H \\ k_{12} & k_{22} \end{bmatrix} \begin{Bmatrix} x \\ y \end{Bmatrix} = \begin{Bmatrix} 0 \\ 0 \end{Bmatrix} \tag{2.6}$$

where the terms k_{ij} in the stiffness matrix depend on the orientation and stiffness of the springs [12]:

$$\begin{aligned} k_{11} &= k_1 \cos^2 \alpha_1 + k_2 \cos^2 \alpha_2 \\ k_{12} &= k_1 \cos \alpha_1 \sin \alpha_1 + k_2 \cos \alpha_2 \sin \alpha_2 \\ k_{22} &= k_1 \sin^2 \alpha_1 + k_2 \sin^2 \alpha_2 + k_H \end{aligned} \tag{2.7}$$

k_H represents the linearized Hertzian contact stiffness [15]; x and y are the vibration displacements in tangential and normal directions. The effect of damping in this system has been studied in [13, 14] and will be briefly discussed below. The most important feature of Eq. (2.6) is that the stiffness matrix is non-symmetric. It can be shown [12] that if the upper diagonal term of the stiffness matrix $k_{12} - \mu k_H \leq 0$, due to the value of friction coefficient μ, the system can become unstable.

To illustrate the mode-coupling mechanism in curve squeal it is convenient to use a modal approach to describe the dynamic properties of the wheel and rail; often modal properties of the wheels are known from finite element (FE) modelling or from modal tests. At least two modes are necessary to initiate this mechanism. Following this idea, as an example Eq. (2.6) has been adopted to represent the two wheel modes summarised in Table 2. These are arbitrarily chosen but represent possible modes encountered in railway wheels. An extensive parameter study is beyond the scope of this review paper but some examples are shown to illustrate some typical features.

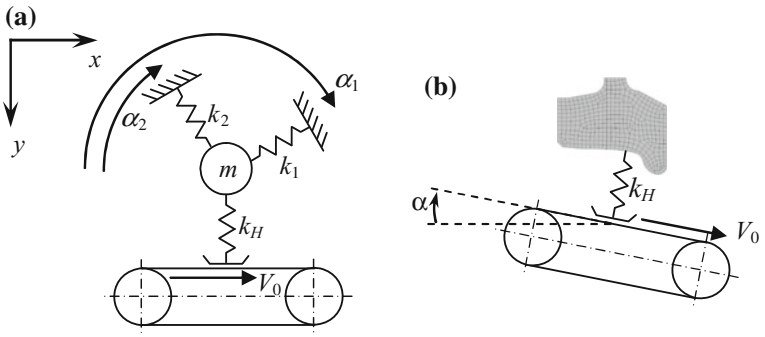

Fig. 5 Two-degree-of-freedom system on moving belt

Table 2 Parameters of a two-modes model of the wheel

	Lowest mode	Highest mode
Natural frequency (Hz)	1983	1993
Modal mass (kg)	0.5	0.5
Mode shape at nominal contact point Normal direction (m)	5.5×10^{-2}	2.7×10^{-2}
Mode shape at nominal contact point Axial direction (m)	2.1×10^{-2}	3.5×10^{-1}
Damping ratio	1×10^{-4}	1×10^{-2}
Rolling velocity (m/s)	2.78	

This approach allows investigation of the effect of the lateral position of the contact point (by adjusting the mode shape parameters) or of the inclination of the contact plane (i.e. the contact angle) between wheel and rail (α in Fig. 5b). Figure 6 shows stability maps obtained for this example by analyzing the real part of the eigenvalues of the system [12]. Results are shown in Fig. 6a for contact on the wheel tread for different values of contact position typical of the leading inner wheel. In this example instability is found for contact positions above 2 mm towards the flange side. Figure 6b shows results for a contact position typical of flange contact for a range of contact angles (40 mm from the nominal position). Here, instability is found for contact angles between 48° and 65° for a friction coefficient of at least 0.4. Although this example is not exhaustive and is given solely for illustrative purposes, it shows that, for these two modes, mode coupling can occur under certain contact conditions and not others.

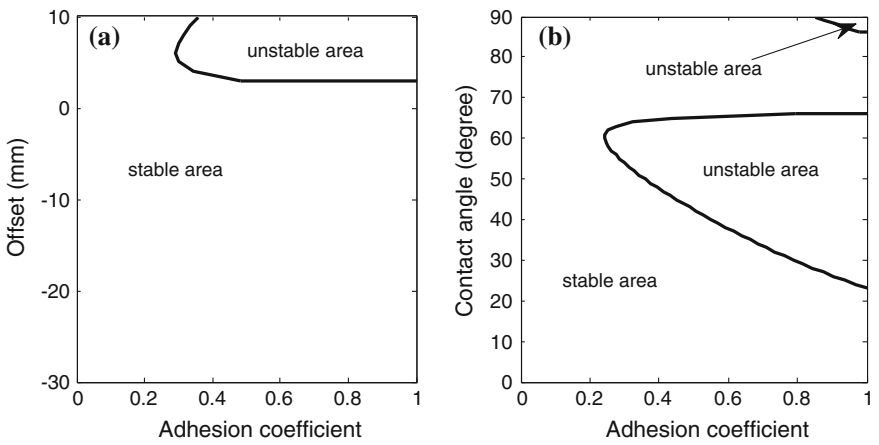

Fig. 6 Stability map for two-mode system with parameters in Table 2: **a** for varying lateral position of the contact and contact angle of 2°; **b** for varying contact angle with a contact position at the wheel flange (40 mm)

Numerical integration of the equations of motion allows the time domain response of the nonlinear system to be obtained. Figure 7a shows the corresponding results obtained with the same two wheel modes. Again the simplified creep force model proposed by Vermeulen and Johnson [9] is adopted, see Fig. 4a, but no negative slope is introduced here. A particular combination of friction coefficient and contact angle in the unstable region is chosen according to the stability map in Fig. 6b, with a value of 50° for the contact angle and 0.6 for the friction coefficient.

An interesting feature of the response due to mode coupling is that both vertical and lateral vibration can increase to a limit cycle and there is a phase lag between the two directions (see Fig. 7b). This phase lag is necessary to transfer the energy from one direction to the other one and generate the instability [12].

The effect of damping in the case of mode coupling is not straightforward [13, 14]; in fact an increase in damping can favour instability in some situations or can improve stability in others. This can be illustrated using the linearized system, again with values from Table 2. Figure 8a shows the stability map for varying friction coefficient when the damping ratio of only the second mode is varied, while the damping ratio of the first mode is kept at 10^{-4}. The system is stable for low values of damping and becomes more unstable when the damping of the second mode is between about 2×10^{-3} and 10^{-1}. Figure 8b shows the stability map when the damping ratios of both modes are increased together while keeping their ratio fixed. In this case changing damping has no effect on the stability up to about 10^{-2}, while the system is quickly stabilised above this value.

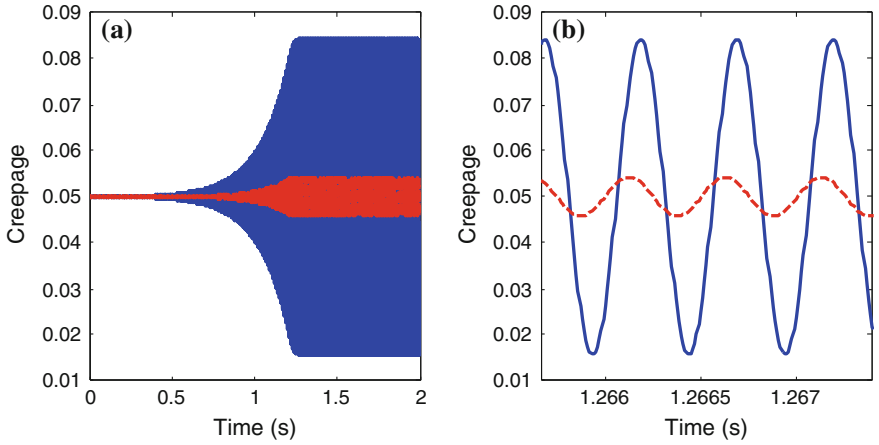

Fig. 7 Time domain solution for a two-mode wheel. **a** Complete solution; **b** close-up in the limit cycle. Red: normal vibration; blue: tangential vibration (shown as creepage or non-dimensional velocity)

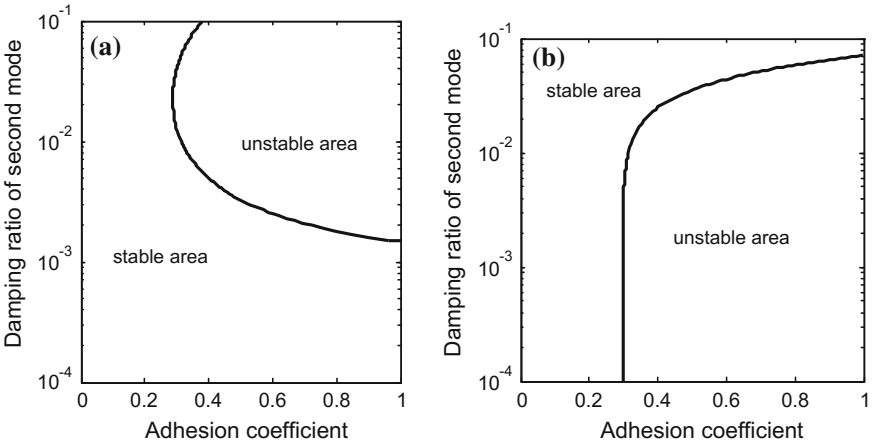

Fig. 8 Stability maps for two-mode system for contact angle 3° and lateral contact position of 8 mm showing effect of damping ratio. **a** Damping ratio of second mode only is varied; **b** damping ratio of both modes is varied, keeping the ratio between them fixed

2.5 Brake Squeal

A related field which has been widely investigated is automotive brake squeal. Kinkaid et al. [16] gave a thorough review of research in this field, and identify a number of potential mechanisms. These were also reviewed by Ghazaly et al. [17]. Stick-slip due to the negative slope of the friction characteristic (see Sect. 2.3) was considered for many years to be an essential ingredient of the brake squeal mechanism but more recent work tends to consider it less important. Other mechanisms discussed include 'sprag-slip' due to geometrically-induced variations in normal force, self-excited vibration under a constant friction coefficient involving mode coupling (as described in Sect. 2.4) and hammering—excitation of disc natural frequencies by impacts between pad and disc. The mode coupling mechanism, in particular between modes of the pad and the disc, is currently the most popular mechanism in brake squeal [17]. Nevertheless it is pointed out that a single mechanism cannot explain all phenomena. Although there are lessons to be learnt from this field for curve squeal, a major difference is that in railway curving the sliding velocities are much smaller than in brake squeal.

Brake squeal modelling often makes use of numerical modelling techniques, representing the disc and pad with finite element models. Ouyang et al. [18] give a review of this approach.

3 Modelling

3.1 Modelling Approaches

There are two main modelling approaches that can be used for curve squeal. In the first, based in the frequency domain, the system is linearized for small fluctuations in friction force about the steady state values and the stability of the linearized system is studied to determine potential unstable frequencies. In the second, the nonlinear equations are solved directly in the time domain.

In curve squeal studies the two most widely used frequency domain methods used to study the stability of the linearized system are complex eigenvalue analysis and the Nyquist criterion. According to the first method the eigenvalues of the system are first calculated and instability is identified when the real part of at least one eigenvalue becomes positive. The growth rate can be identified from the real part of the eigenvalue. In the second case the system is described by a feedback loop with positive feedback and the Nyquist criterion [19] is applied to the open loop transfer function. The open loop transfer function is plotted on the complex plane and if it encloses the point (+1,0) the system is unstable. In addition, by plotting the magnitude of the open loop transfer function against frequency, the frequencies associated with these unstable points can be identified as likely squeal frequencies. The two methods essentially give similar information: the growth rate is proportional to the ratio of the loop gain to the modal mass of the corresponding mode [20]. Both can give multiple unstable frequencies; the one which will dominate the squeal response depends on the initial conditions as well as the respective growth rates and cannot be determined using these frequency domain methods.

Time domain methods allow the evolution of the response to be determined and the limit cycle amplitude to be obtained taking full account of the system nonlinearities. The calculation effort is much greater, especially for a detailed model of the wheel and track, and this method is therefore more difficult to use in parametric investigations. Nevertheless, with the improvement in computational speed these methods are being used more widely.

3.2 Wheel Dynamic Behaviour

The wheel dynamic behaviour is an important component of curve squeal. In particular, squeal is usually associated with lightly damped modes of vibration of the wheel. Each mode has a harmonic variation in amplitude around the circumferential direction, which can be categorized according to the number of nodal diameters, n [7]. Example modeshapes are shown in Fig. 9 for a wheel with diameter 0.84 m. These modes are for $n = 2$, but for other values of n the cross-section of the modeshape is similar. Axial modes can be identified according

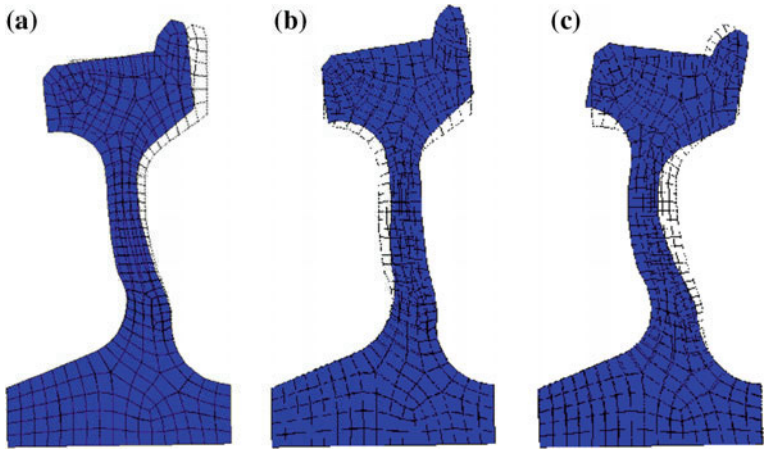

Fig. 9 Examples of mode shapes of Class 15x wheel with $n = 2$. **a** 0-nodal-circle axial mode (2,0), 463.0 Hz; **b** radial mode (2,R), 2220 Hz; **c** 1-nodal-circle mode (2,1), 2901 Hz

to the number of nodal circles m and will be identified as mode (n,m). Additionally radial (n,R) and circumferential (n,C) modes occur [7].

The natural frequencies of the various mode types of this wheel are plotted in Fig. 10 against the number of nodal diameters, n. Measured values are plotted using a solid line and, where these could not be identified, corresponding results from finite element calculations are supplied using a dotted line. Generally curve squeal occurs most often in one of the 0-nodal-circle axial modes which have a large axial component at the wheel/rail contact point and small radial component but, as will be seen, in some situations other mode types are excited. For a monobloc steel wheel, the damping ratio of these axial modes is of the order of 10^{-4} for $n \geq 2$. For $n = 1$ the modes are strongly coupled with the axle bending and are therefore much more strongly damped due to the bearings. Similarly for $n = 0$ the modes are coupled with axle extension or torsion.

3.3 *Models Based on Falling Friction*

Rudd [3] developed an early model of curve squeal, based on excitation by lateral creepage at the wheel/rail contact with instability induced by falling friction in the saturated region, a mechanism first suggested by von Stappenbeck [21]. Rudd's approach was based on the concept of negative damping introduced by the falling friction characteristic; the wheel was represented by a single mode. Rudd's model was also adopted by van Ruiten [22] in an investigation of the squeal noise of trams.

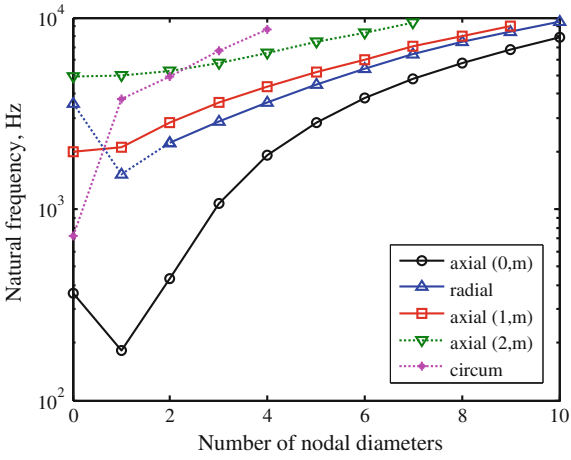

Fig. 10 Natural frequencies of Class 15x wheel, diameter 0.84 m. Solid line measured; dotted line calculated

Nakai et al. [23–25] developed a model in which a stationary steel disc (representing the wheel) is rubbed by a moving rod (representing the rail). This theoretical study shows that squeal noise frequency usually relates to one wheel axial mode with a small damping value. Contact load and contact position were found to have an effect on the occurrence of squeal noise.

Schneider et al. [26] modelled the wheel analytically as a disc and its sound radiation using a Rayleigh integral. They used Kraft's friction model [27] (see Sect. 4.1.1) and solved the non-linear equations of motion in the time domain. Only the axial 0-nodal-circle modes were included in the calculation; the response was found to contain multiple modes. Fingberg [28] extended the model of Schneider et al. [26] to use a finite element model of the wheel, a dynamic model of the track and a boundary element model for the sound radiation. This was again solved in the time domain. The dominant frequency was found to vary with the rolling velocity. This work has been extended further by Périard [29] who also included the vehicle curving behaviour in the same time-stepping calculation procedure as the squeal model.

Heckl and Abrahams [30] presented a simple time-domain model based on the impulse response of a disc, representing the wheel. The lateral friction force was considered as a piecewise linear function with a falling region at large relative velocities and a rising region at small creepages. They showed that the non-linear friction force leads to a limit cycle response, and this limit cycle frequency is determined by one unstable mode of the wheel. Axial modes (2,0) and (3,0) were both unstable but the limit cycle consists of one of these modes, depending on the conditions. Heckl [31, 32] also presented a frequency-domain model of the same disc which allowed the growth rate and frequency of the squeal to be determined and its dependence on the damping loss factor of the disc to be determined. Measurements were presented of the squeal of this simple disc running on a rotating turntable.

Liu and Meehan [33, 34] recently developed a simple single-degree-of-freedom model for curve squeal which neglects vertical dynamics (so no mode coupling is possible) and relies on the negative slope of the friction curve as the source of instability. This is used to explain the increase in sound level with rolling speed and with angle of attack found in a test rig. In their tests, peaks were found corresponding to the axial modes with $n = 3$, 4, 5 and 6.

3.4 Inclusion of Vertical Dynamics

De Beer et al. [20, 35, 36] developed a model for squeal noise in the frequency domain, which combines models of wheel dynamics, rail dynamics and contact dynamics in the vertical and lateral directions. For wheel and rail dynamics, mobilities obtained from the TWINS software [37] were used. For the contact dynamics in the vertical direction, a contact spring mobility was adopted, while for the lateral contact dynamics the creepage at low sliding velocities was calculated using the model of Shen et al. [10] and a falling region was introduced using the model of Kraft [27]. The Nyquist criterion was used to assess the stability of the system in the frequency domain. Unstable frequencies were found corresponding to 0-nodal-circle axial modes with between 2 and 6 nodal diameters. This model appears to be the first in which the variation of the normal contact force was included in a curve squeal model. Although this will potentially introduce mode-coupling phenomena, this possibility was not considered explicitly in this paper and from measurements the presence of squeal was associated with a falling friction curve. The model showed the importance of the lateral position of the contact point on the wheel.

Monk-Steel and Thompson [38] extended de Beer's model to include varying longitudinal and spin creepage as well as lateral creepage and normal load variations. Again only the falling friction aspect was considered. The model was presented in the form of a flow diagram as shown in Fig. 11. The upper part represents the excitation due to falling friction, where [G] contains the mobilities of the wheel and rail system and $[H_1]$ contains terms from the contact mechanics including the slope of the adhesion coefficient. The term $[H_2]$ represents the influence of the

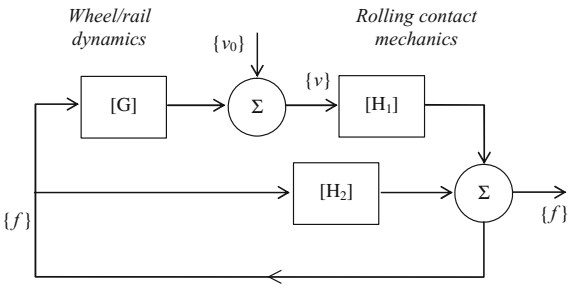

Fig. 11 Feedback loop for squeal model [38]

normal load variations on the transverse forces. The open loop transfer function is given by $H_1G + H_2$ [11]. In the case where longitudinal and spin creepage are included this feedback loop involves matrices and the generalised Nyquist criterion is used based on the eigenvalues of the open loop transfer function matrix [39]. For a contact point on the wheel tread, squeal was predicted to occur in the 0-nodal-circle axial modes with various numbers of nodal diameters.

Huang [11, 40] also used this approach to extend de Beer's model to include all possible degrees of freedom in the wheel/rail contact and compared results with measurements obtained on a test rig [41]. A heuristic formula for falling friction at large creepages was introduced and combined with the FASTSIM model for rolling contact [8]. Both frequency-domain and time-domain approaches were considered and compared. A parametric study was carried out, which included changing the steady-state creepages, contact position and contact angle. An extension of this model to include the effect of a second contact point was developed following this approach by Squicciarini et al. [42]. They also considered a statistical approach in which the model was run for a large number of cases in which various parameters were selected from a statistical distribution.

Xie et al. [43] introduced into SIMPACK a modified version of FASTSIM including falling friction as developed by Giménez et al. [44] so that the curving analysis would be consistent with the squeal model.

Chiello et al. [45] developed a squeal model that considered normal contact dynamics. The wheel dynamics was derived from a modal basis. The friction force used included a falling part, linearly decreasing with speed after saturation, which can induce instability. It was pointed out that the asymmetry of the stiffness matrix, leading to mode coupling, can be another possible source of instability but this was believed not to be important by the authors in this particular case and was found to occur only with large lateral offset of the contact point. The modal growth rate was obtained as a measure of stability, which showed that the model could only be destabilised by negative damping. Squeal was predominantly found in the (3,0) axial mode at around 1.1 kHz. However, it was found that the dominant mode can be different if different initial conditions are considered, and if harmonically-related modes are present they can coexist in the limit cycle. Collette [46] investigated the influence of vertical dynamics and showed that, even with a constant friction coefficient, this could lead to unstable vibration.

Brunel et al. [47] performed a transient analysis of a wheel using an axi-harmonic finite element model. Two friction laws were considered based on measurements from Kooijman et al. [35], one with a falling characteristic and one with an increasing friction force. It was found that even the positive friction law could lead to a limit cycle solution, which the authors identified with the coupling of the normal and lateral dynamics of the wheel (which they misleadingly refer to as sprag-slip). Nevertheless, it was found that the falling friction characteristic led to much higher levels of squeal. Squeal was found to occur in axial modes with $n = 3$, 4 and 5 between 1 and 3 kHz.